Numerical Investigations of the Keiper-Li Criterion for the Riemann Hypothesis

Ross McPhedran[1,*]

[1] School of Physics, University of Sydney 2006, Australia,
ross.mcphedran@sydney.edu.au

April 16, 2024

Abstract

The Keiper-Li criterion gives a necessary and sufficient condition for the Riemann hypothesis. It requires that a set of quantities λ_n be positive, and involves auxiliary constants a_n, known to be positive. A recently derived expression for the a_n is used to provide accurate numerical values for the first four thousand a_n's, and asymptotic expressions together with bounds for them are investigated.

1 Introduction

The long history of research into the Riemann hypothesis has featured many advances in mathematical techniques and approaches. Among these, we concentrate on that of Keiper [1] and Li [2]. In independent work, they published investigations into the connection between the Riemann hypothesis and the properties of sums over reciprocal powers of zeros of the Riemann zeta function, whose symmetrised form is $\xi(s)$. Denoting the zeros of $\xi(s)$ by ρ, the Riemann hypothesis is that $\Re(\rho) = 1/2$. Both Keiper and Li related the Riemann hypothesis to the positivity of certain expansion coefficients λ_n pertaining to ξ. Representing the λ's of the two authors by respectively λ^K and λ^L and using Li's definition from [2], we have:

$$(n-1)!\lambda_n^L = \frac{d^n}{ds^n}\left[s^{n-1}\log(2\xi(s))\right]_{s=1} = n!\lambda_n^K, \tag{1}$$

so $\lambda_n^L = n\lambda_n^K$.

The connection between the Riemann hypothesis and the λ's is made clear by the following equation:

$$\lambda_m^L = m\lambda_m^K = \sum_\rho \left[1 - \left(\frac{\rho}{\rho-1}\right)^m\right]. \tag{2}$$

If each ρ has real part of one half, then the quantity in round brackets in (2) has modulus unity, and the sum over conjugate pairs of roots must then be positive. If any root has a real part in excess of one half, then it contributes a term with modulus in excess of unity, whose mth power goes to infinity with m. Keiper provided the first two terms in a large m expansion of λ_m^K, based on assuming the Riemann hypothesis and assuming what he described as "very evenly distributed" zeros:

$$\lambda_m^K \approx \frac{1}{2}\log m - \frac{1}{2}(\log(2\pi) + 1 - \gamma). \tag{3}$$

Note that the assumption of an even distribution of zeros has been proved unnecessary [3, 4]. More results of Keiper and some extensions of them are given in a recent article by McPhedran, Scott and Maignan [5], to which we will refer frequently here.

Li's paper [2] was written in a more formal style than Keiper's. It contains the following important result:

Theorem 1. *(Li) A necessary and sufficient condition for the nontrivial zeros of the Riemann zeta function to lie on the critical line is that λ_n^L is non-negative for every positive integer n.*

Li [2] defines a set of coefficients a_j through the equation

$$\phi(z) = 2\xi\left(\frac{1}{1-z}\right) = 1 + \sum_{j=1}^{\infty} a_j z^j, \tag{4}$$

and is able to show that all of these are positive. Li then connects the λ_n^L and the a_n in the following recurrence relation:

$$\lambda_n^L = n a_n - \sum_{j=1}^{n-1} \lambda_j^L a_{n-j}. \tag{5}$$

The main purpose of this paper is to detail how Li's coefficients a_n may be calculated in an accurate way, and to give values for the first four thousand of them. We will also provide early results on asymptotic expressions for the a_n, and investigate the nature of their connection with the λ_n.

2   Evaluation of the constituents of the a_n

It is the purpose of the work presented here to describe investigations into an alternative approach to the calculation of the Keiper-Li sequence, with the hope that the elusiveness and ill-conditionedness encountered by previous workers may be reduced. The alternative approach replaces the basis of sums σ_k (which fluctuate irregularly in sign as k increases) with the basis of derivatives ξ_r of $\xi(s + 1/2)$ around $s = 0$. It is important that all the coefficients ξ_r are positive,

as proved by Pustyl'nikov [6], a fact known to Hurwitz and Jensen. (The first author is indebted to J. Gélinas for this comment.)

We will evaluate the a_n's using the following expansion coefficients ξ_r. These occur in the expansion of $\xi(\tilde{s} + 1/2)$, based on the work of Pustyl'nikov [6, 7] and Hadamard [8]:

$$\xi\left(\tilde{s} + \frac{1}{2}\right) = \sum_{r=0}^{\infty} \xi_r \tilde{s}^{2r}, \tag{6}$$

where the coefficients ξ_r can be obtained in integral form from

$$\xi_r = \frac{2^{-(2r+2)}}{(2r)!} \mathcal{I}_{2r}, \tag{7}$$

with

$$\mathcal{I}_r = \int_1^{\infty} [\log(x)^{r-2}][16r(r-1) - \log(x)^2]x^{-3/4}\omega(x)dx \tag{8}$$

and $\omega(x) = \sum_{n=1}^{\infty} \exp(-\pi n^2 x)$ being related to the elliptic theta function ϑ_3. Pustyl'nikov [7] establishes in his Theorem 1 that all even order derivatives of $\xi(s)$ at $s = 1/2$ are strictly positive. His Theorem 2 is that Theorem 1 provides a necessary condition for the Riemann hypothesis to hold. Asymptotic analysis of the integral (6) may be found in Pustyl'nikov [6], while the author has benefited from a valuable communication of Jacques Gélinas [9]. The latter reference contains extensions to the asymptotics of Pustyl'nikov, which give an accurate exponent and first digit for the ξ_r. Recent publications [10, 11] contain formulae which substantially improve the asymptotic analysis, such that 16-18 decimal digits are given for r in the range 2000-20000.

The ξ's enter into the formula from [5] via sums over an integer r containing ξ_r and r^p for p a positive integer:

$$\Sigma_p^{\xi} = \sum_{r=1}^{\infty} \frac{\xi_r}{2^{2r}} r^p. \tag{9}$$

2.1 Evaluation of the sums Σ_p^{ξ}

The investigations into the sums Σ_p^{ξ} reported here relied on a tabulation of highly accurate values (1000D) for the ξ_r calculated by R. Kreminski [12]. The first 500 of these were taken several years ago by the author from an on-line public data base, now under reconstruction. They have been used with truncation to either 100 or 200 decimal places.

In the paper [5] an asymptotic expansion for the summand (a function of the integer variable r) of the Σ_p^{ξ} is derived, using results of Pustyl'nikov [6], [7], Hadamard [8], Griffin, Ono, Rolen and Zagier [10], and O'Sullivan [11]. The summand is maximised in the asymptotic region when $r = r_m$, where to leading order:

$$\frac{p}{2r_m} - \log(4\pi) = W\left(\frac{2r_m}{\pi}\right). \tag{10}$$

Here W denotes the W function of Lambert, which is positive for $r > 0$. Hence, p/r_m must be larger than $2\log(4\pi) \approx 5.06204$. The connection we require is the inverse of this: r_m as a function of p. This inversion can be achieved using generalised Lambert functions [13, 14]. Denoting the generalized Lambert W function according to [13, eq.28] as $\Omega_2(0, -\ln(4\pi))$ the solution for r_m is exactly [5]:

$$r_m \;=\; \frac{p}{2(\ln(4\pi) + \Omega_2(0, -\ln(4\pi)))} \;. \tag{11}$$

This formula has been shown to furnish values up to very large values ($p = 10^{40}$).

Using the Kreminski values truncated to 200 decimal places for the first 500 ξ_r's, we have evaluated the sums Σ_p^ξ up to $p = 4000$. The summands for $p = 2000$ and $p = 4000$ are shown in Figs. 1 and 2, in normalised form. For each, the summand has been divided by its maximum value: for $p = 2000$, the base ten logarithm of this is 3685.774, while for $p = 4000$ it is 8432.102. As commented in [5], near the maximum the summand can be well approximated by a Gaussian form, but for these large values of p, well away from the maximum the summand slopes less rapidly for r above r_m than for r below it. The contrast between the maximum value and that at the right-hand edge of the graph is a factor of 10^{920} for $p = 2000$, and 10^{268} for $p = 4000$. This demonstrates that summing over 500 zeros is still adequate, even for $p = 4000$.
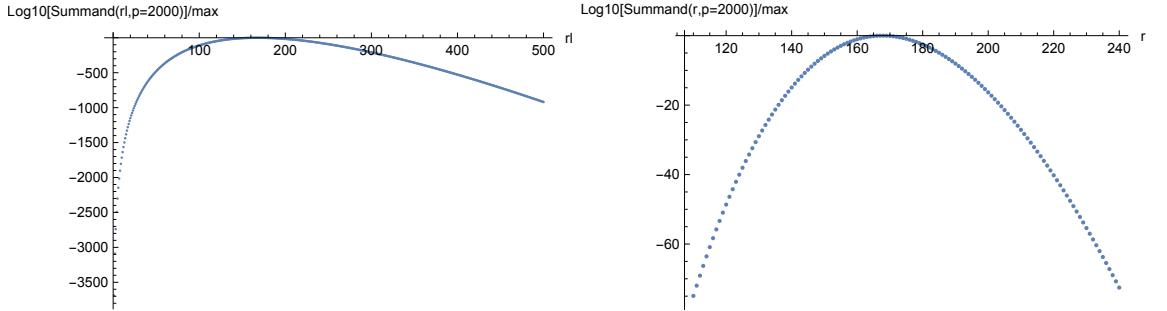

Figure 1: The logarithm (base ten) of the summand for Σ_p^ξ, $p = 2000$, divided by its maximum value. The two plots are for all values (left) and for the region near the maximum (right)

In Fig. 3 we show the value of r, r_m, maximising the summand in Σ_p^ξ for p ranging from 10 to 4000. The data points are compared with an approximate formula from [5]:

$$r_m = \frac{p}{2(\log(4\pi) + z)}, \quad z \approx \log\left(\frac{p}{\pi([W(\sqrt{p}) + W(\sqrt{p/(2\sqrt{\pi})}]^2 - \log(2\sqrt{\pi})^2))}\right). \tag{12}$$

We next construct a quite accurate asymptotic estimate for the sums Σ_p^ξ based on the estimates provided in [5], equations (120) and (124). The second
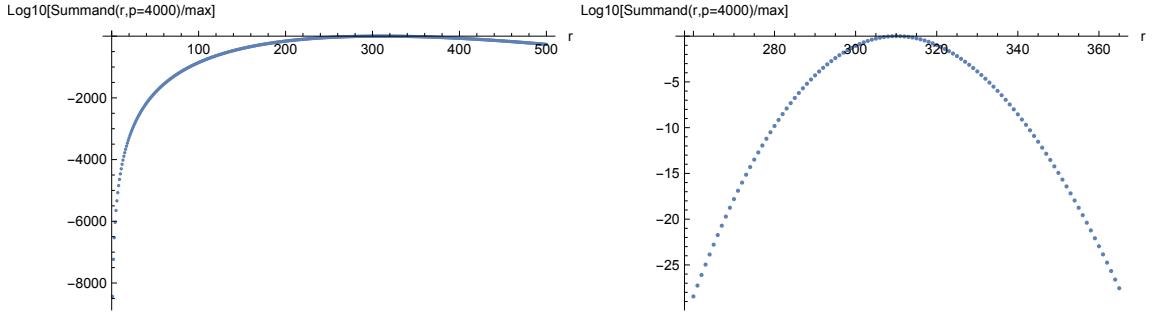
Figure 2: The logarithm (base ten) of the summand for Σ_p^ξ, $p = 4000$, divided by its maximum value. The two plots are for all values (left) and for the region near the maximum (right)
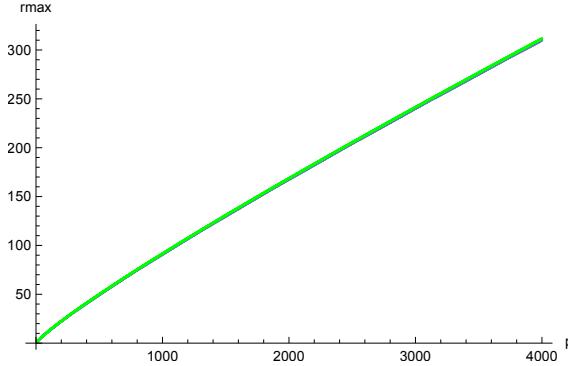

Figure 3: The value of r, r_m, which maximizes the summand of Σ_p^ξ as a function of p. The highly accurate data values (blue) are compared with the approximate formula (12), shown in green. The two agree to graphical error for the range of p from 10 to 4000.

of these gives an expression for the dominant contribution to the exponent:

$$S_1(n_m, p) \approx p \left[\log p - \log \log p - 2 + \frac{2 \log \log p}{\log p} - \frac{\log(4\pi^2)}{\log p} \right]. \qquad (13)$$

We truncate this to form an expression which can be used with FindFit to give estimates for $\log \Sigma_p^\xi$ from sets of numerical values for it, ranging up to one running from $p = 10$ to $p = 4000$. The expression is:

$$\log \Sigma_p^\xi \approx p[L_1 \log p - L_2 \log \log p - L_3]. \qquad (14)$$

For $p = 10 - 1000$ the results are: $L_1 \approx 0.882615116$, $L_2 \approx 0.078960314$ and $L_3 \approx 2.306757511$. For $p = 10 - 2000$ the results are: $L_1 \approx 0.9035396927$, $L_2 \approx 0.207352057$ and $L_3 \approx 2.202830417$. For $p = 10 - 4000$ the results are:

5

$L_1 \approx 0.920627926$, $L_2 \approx 0.324243018$ and $L_3 \approx 2.095391955$. The movement of these towards what we might expect from (13) is slow, in keeping with the likely logarithmic nature of the asymptotic trends.

In each of the three cases, the graphs of $\log \Sigma_p^{\xi}$ and of the right-hand side of (14) versus p agree to graphical accuracy. The graphs of the two and their difference are given in Fig. 4.
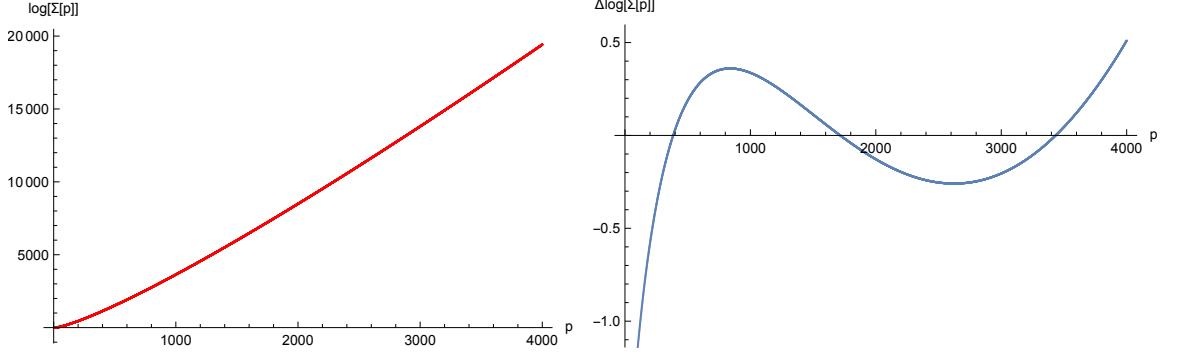

Figure 4: (Left) Accurate values of $\log \Sigma_p^{\xi}$ (blue) are compared with values from the asymptotic approximation in (14) (red).The two agree to graphical error for the range of p from 10 to 4000. (Right) The difference of the two values sets as a function of p.

2.2 Evaluation of the expansion coefficients $\mathcal{C}(n,p)$

The coefficients $\mathcal{C}(n,p)$ arise via the following expansion:

$$\left(\frac{1+w}{1-w}\right)^r = 1 + \sum_{n=1}^{\infty} a_r(n)w^n. \tag{15}$$

Here the coefficients $a_r(n)$ are explicit:

$$a_r(n) = \sum_{p=0}^{n} \binom{r+n-p-1}{r-1}\binom{r}{p}. \tag{16}$$

The $a_r(n)$ are polynomials in r of degree n. We note that they occur in the discussion of the coordination sequences for n dimensional cubic lattices, of interest in crystallography [15, 16]. Some particular examples are to be found in [17]: A008412, A008414, A008416. The first four are $4r$, $8r^2$, $4r/3 + 32r^3/3$ and $16r^2/3 + 32r^4/3$.

The coefficients of the powers of r in these polynomials are the $\mathcal{C}(n,p)$:

$$a_{2r}(n) = \sum_{p=1}^{n} \mathcal{C}_{n,p}r^p. \tag{17}$$

6

the coefficients $\mathcal{C}_{n,p}$ satisfy the general recurrence relation:

$$\mathcal{C}_{n,p} = \frac{4}{n}\mathcal{C}_{n-1,p-1} + \frac{(n-2)}{n}\mathcal{C}_{n-2,p}, \text{ for } 1 \leq p \leq (n-2). \tag{18}$$

They also exhibit a sum property:

$$\sum_{p=1}^{n}\mathcal{C}_{n,p} = 4n. \tag{19}$$

Exact values of the $\mathcal{C}(n,p)$ for n up to 20 are given in [5].

The values of $\mathcal{C}_{n,p}$ were calculated in Mathematica with an accuracy set at 200 digits. These were used to calculate Gaussian fits using the FindFit function, with starting points for the fit based on the maximum value for $\mathcal{C}_{n,p}$ for the given n with p varying in the table, and the value of p for which it occurred. This was done for each n in the range 10 to 4000. An example of the tabled and fitted points is given in Fig. 5 for $n = 4000$. The Gaussian model agrees well with the tabulated points, but generates a better estimate for the location and height of the maximum and its width than does the table (the latter of course being limited to a resolution of unity in p).
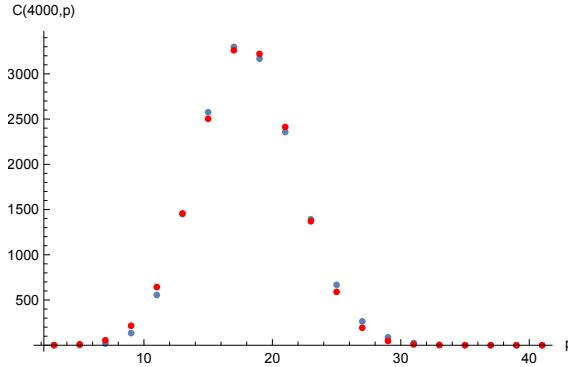

Figure 5: Values of $\mathcal{C}(n,p)$ for $n = 4000$ with p varying (blue dots)) are compared with the Gaussian model from FindFit (red dots).

The Gaussian model used was of the form:

$$\mathcal{C}(n,p) = A_o \exp\left[\frac{-(p - B_o)^2}{C_o}\right]. \tag{20}$$

For the fit shown in Fig. 5, the parameters were (in truncated form): $B_o = 17.910980$, $A_o = 3355.409138$ and $C_o = 28.922582$. Note that the parameters A_o and C_o can be linked using the exact result (19). Indeed, Also, if we evaluate the integral of equation (20) over p and compare the result with the exact relation (19), bearing in mind that the $\mathcal{C}(n,p)$ are zero if the (n,p) are an even-odd or

odd-even pair, we find

$$A_o \approx \frac{8n}{\sqrt{\pi C_o}}, \; C_o \approx \frac{1}{\pi}\left(\frac{8n}{A_o}\right)^2. \tag{21}$$

For the case quoted above, using A_o as quoted we find for C_o the estimate 28.950703.

The fit parameters $A_o(n), B_o(n), C_o(n)$ were evaluated for n in the range 100 to 4000. Figure 6 shows the two estimates for C_o (direct and from equation (21) agree over this whole range to graphical accuracy, with the relative accuracy being around 10^{-3}. Using (21) we write the expression (20) as
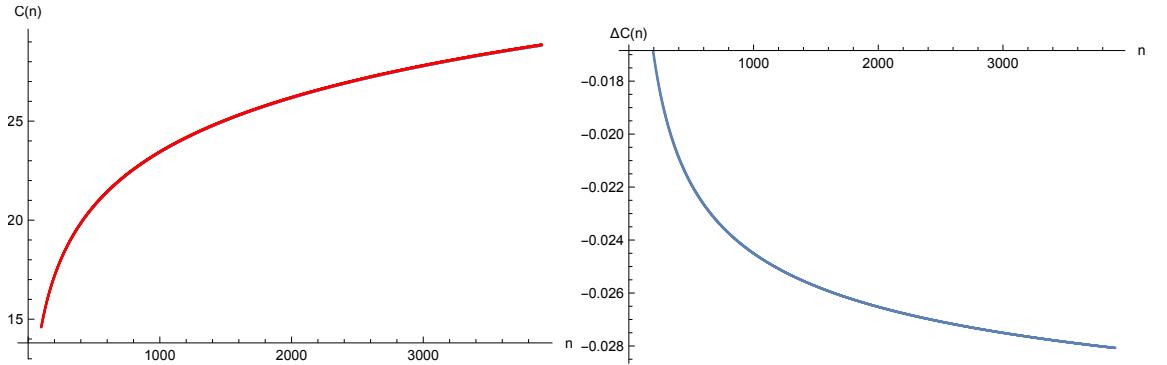

Figure 6: (Left) The fit parameter C_o directly calculated (blue) is compared at left with that obtained from A_o using equation (21) (red) for n ranging from 100 to 4000. The two agree to graphical accuracy. (Right) The difference between the two values of C_o is plotted.

$$\mathcal{C}(n,p) \approx A_o \exp\left[-\pi\left(\frac{(p-B_o)}{8n/A_0}\right)^2\right]. \tag{22}$$

The position B_0 of the maximum of $\mathcal{C}(n,p)$ with p varying is well described by the following expression obtained using FindFit:

$$B_o \approx 1.968480 \log n + 1.577877, \tag{23}$$

The variation of A_o with n has the dominant factor n. To model accurately this parameter, we study the quantity n/A_o as a function of $\log n$. The dominant terms correspond to a linear form, but a good approximation is obtained with the addition of a term in $1/\log(n)$. The result from FindFit is:

$$\frac{n}{A_o} \approx 0.066472413 \log n + 0.78108997 - \frac{1.16130124}{\log n}. \tag{24}$$
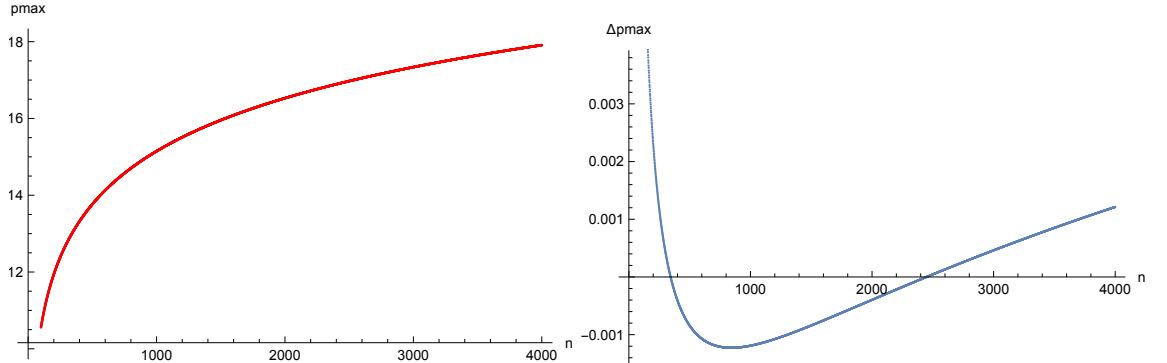
8

Figure 7: (Left) The fit parameter B_o directly calculated (blue) is compared at left with that obtained from the representation (23) (red) for n ranging from 100 to 4000. The two agree to graphical accuracy. (Right) The difference between the two values of B_o is plotted.

We can deduce the dominant term in the variation of A_o with n based on a differential approach to the recurrence relation (18), valid when n and p are both large. We use the following approximations:

$$\mathcal{C}(n-1, p-1) = \mathcal{C}(n, p) - \frac{\partial \mathcal{C}(n, p)}{\partial n} - \frac{\partial \mathcal{C}(n, p)}{\partial p}, \qquad (25)$$

and

$$\mathcal{C}(n-2, p) = \mathcal{C}(n, p) - 2\frac{\partial \mathcal{C}(n, p)}{\partial n}. \qquad (26)$$

Substituting these in (18), we find:

$$\frac{\partial \mathcal{C}(n, p)}{\partial p} = \frac{1}{2}\left(\mathcal{C}(n, p) - n\frac{\partial \mathcal{C}(n, p)}{\partial n}\right). \qquad (27)$$

Hence,

$$\frac{\partial \mathcal{C}(n, p)}{\partial p} = 0 \implies \mathcal{C}(n, p) = n\frac{\partial \mathcal{C}(n, p)}{\partial n}. \qquad (28)$$

Thus, the maximum value of $\mathcal{C}(n, p)$, $A_o(n)$, must have as its leading term a constant term multiplying n, as in (24).

Note that the asymptotic formulae of this section require $\log n$ to be large. This provides a motivation to extend the studies made here to much larger values of n than 4000, thus securing more accurate expansions of A_o and B_o. Given the small value of the coefficient of $\log(n)$ in $A_0(n)$, we require n in the range of $10^5 - 10^6$ to enter fully into the asymptotic region.
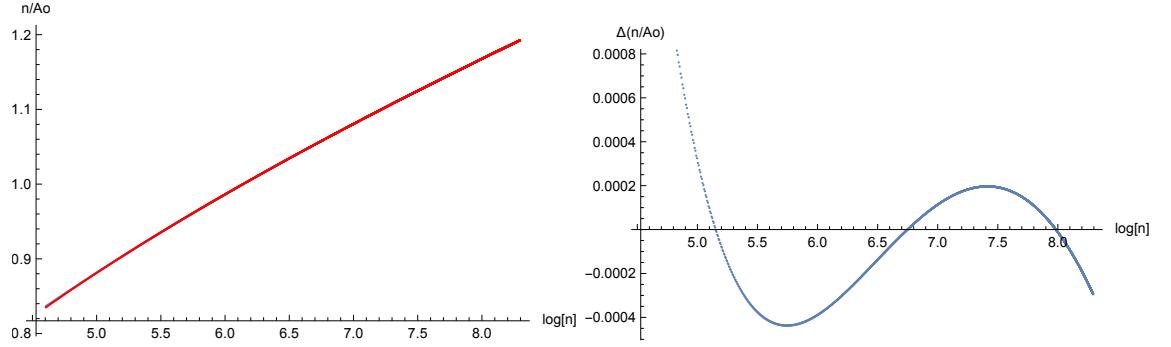
9

Figure 8: (Left) The fit parameter n/A_o directly calculated (blue) is compared at left with that obtained from the representation (24) (red) for the abscissa $\log n$, with n ranging from 100 to 4000. The two agree to graphical accuracy. (Right) The difference between the two values of n/A_o is plotted.

2.3   A Pair of Recurrence Relations for the $\mathcal{C}(n,p)$

The recurrence relation we now discuss works with a set of $\mathcal{C}(n,p)$ with a given p, and generates the successor set for $p+1$. The first set is for $p=1$:

$$\mathcal{C}_{2n-1,1} = \frac{4}{2n-1}. \tag{29}$$

One way of expressing the set for $p=2$, $\mathcal{C}_{2n,2}$, is in terms of harmonic numbers, where the nth harmonic number H_n is defined by [18]:

$$H_n = \sum_{k=1}^{n} \frac{1}{k}. \tag{30}$$

We then have:

$$\mathcal{C}_{2n,2} = \frac{8}{n}\left[H_{2n} - \frac{1}{2}H_n\right]. \tag{31}$$

We can re-express (31) using the following multiplication formula for $H(n)$:

$$H_{2n} = H_n + \sum_{k=1}^{n} \frac{1}{2k(2k-1)} = H_n + \mathcal{H}_1(n), \tag{32}$$

where, using the properties of the digamma function,

$$\mathcal{H}_1(n) = \log 2 + \frac{1}{2}\left[\psi\left(n+\frac{1}{2}\right) - \psi(n+1)\right]. \tag{33}$$

Here $\mathcal{H}_1(n)$ has the expansion:

$$\mathcal{H}_1(n) = \log(2) - \frac{1}{4n} + \frac{1}{16n^2} - \frac{1}{128n^4} + \frac{1}{256n^6} - \frac{17}{4096n^8} + \frac{31}{4096n^{10}} + O\left((1/n)^{11}\right), \tag{34}$$

10

so that it tends to $\log 2$ as n tends to infinity. Hence, (31) is

$$\mathcal{C}_{2n,2} = \frac{4}{n}H_n + \frac{8}{n}\mathcal{H}_1(n). \tag{35}$$

The recurrence relations start with (29) and (35). One goes from p even to p odd:

$$\mathcal{C}_{2n-1,2q-1} = \frac{4}{2n-1}\sum_{k=q-1}^{n-1}\mathcal{C}_{2k,2q-2}. \tag{36}$$

The other goes from p odd to p even:

$$\mathcal{C}_{2n,2q} = \frac{4}{2n}\sum_{k=q}^{n}\mathcal{C}_{2k-1,2q-1}. \tag{37}$$

Each relation involves a sum beginning with $\mathcal{C}_{n,n} = 4^n/n!$.

Useful references giving expressions for sums over harmonic numbers are [19]-[23]. From [23], an alternative expression to (35) is :

$$\mathcal{C}_{2n,2} = \frac{8}{n}\left[\frac{3}{2}H_n - \frac{1}{\binom{2n}{n}}\sum_{k=0}^{n}\binom{n}{k}^2 H_k\right]. \tag{38}$$

The convention here is $H_0 = 0$.

We now use the expression (35) to evaluate asymptotically $\mathcal{C}_{2k-1,3}$, using [20]:

$$\sum_{k=1}^{n-1}\frac{H_k}{k} = \frac{1}{2}H_{n-1}^2 + \frac{1}{2}H_{n-1}^{(2)}, \tag{39}$$

an expression involving the second order harmonic number, denoted here as $H_n^{(2)}$, with in general :

$$H_n^{(p)} = \sum_{k=1}^{n}\frac{1}{k^p}. \tag{40}$$

Then:

$$\mathcal{C}_{2n-1,3} = \frac{16}{2n-1}\left[\frac{1}{2}H_{n-1}^2 + \frac{1}{2}H_{n-1}^{(2)} + 2\sum_{k=1}^{n-1}\frac{\mathcal{H}_1(k)}{k}\right]. \tag{41}$$

We seek next to evaluate the first two leading terms in the expansion of the sum of $2\mathcal{H}_1(k)/k$ in equation (41). The first of these is $2\log(2)H_{n-1}$, which diverges as $n \to \infty$. The second is a negative constant, which we evaluate by direct summation up to a chosen integer n_s, and then summation of the asymptotic series in (41) from n_s+1 to infinity, using the Hurwitz zeta function, with result:

$$-\frac{\zeta(2,n_s+1)}{2} + \frac{\zeta(3,n_s+1)}{8} - \frac{\zeta(5,n_s+1)}{64} + \frac{\zeta(7,n_s+1)}{128} - \frac{17\zeta(9,n_s+1)}{2048}$$
$$+\frac{31\zeta(11,n_s+1)}{2048} + O\left((1/n_s)^{13}\right). \tag{42}$$

11

This procedure gives for the negative constant the value -0.68402303904307344131. The results for $n_s = 100$ and $n_s = 500$ agree to all digits quoted.

Using the result from (42), we obtain the following expression:

$$\frac{(2n-1)\mathcal{C}_{2n-1,3}}{4} = 2H_{n-1}^2 + 8\log(2)H_{n-1} + 2H_{n-1}^{(2)} - 4 \times 0.68402303904307344131.$$
(43)

In Fig. 9 we show that this formula agrees with the exact results to graphical accuracy, and that the difference between the two tends to zero as increases. That difference is 0.002 for $n = 1000$.
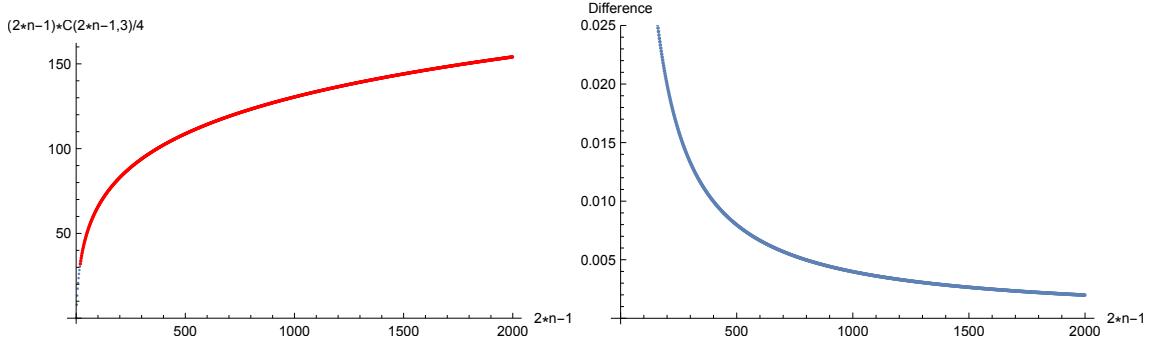

Figure 9: (Left) The exact $(2n-1)\mathcal{C}_{2n-1,3}/4$ values (blue) are compared with those from the fit function (red) . The two agree to graphical accuracy. (Right) The difference between the two values is plotted.

A second way of evaluating the negative constant found above proceeds through a class of sums $\mathcal{H}_p$ defined as follows:

$$\mathcal{H}_p(n) = \sum_{k=1}^{n} \frac{1}{(2k)^p(2k-1)}.$$
(44)

Then

$$\mathcal{H}_p(n) = \sum_{k=1}^{n} \frac{1}{(2k)^{p-1}(2k-1)} - \sum_{k=1}^{n} \frac{1}{(2k)^p} = \mathcal{H}_{p-1}(n) - \frac{H_n^{(p)}}{2^p}.$$
(45)

Hence,

$$\mathcal{H}_p(n) = \mathcal{H}_1(n) - \sum_{q=2}^{p} \frac{H_n^{(q)}}{2^q}, \quad \mathcal{H}_1(n) = \mathcal{H}_p(n) + \sum_{q=2}^{p} \frac{H_n^{(q)}}{2^q}.$$
(46)

Taking the limit as n tends to infinity:

$$\lim_{n \to \infty} \mathcal{H}_p(n) = \log(2) - \sum_{q=2}^{p} \frac{\zeta(q)}{2^q}.$$
(47)

12

As $p \to \infty$, the right-hand side of (47) tends to zero.

The right-hand side equation in (46) may be used to evaluate $\mathcal{H}_1(n)$ to high accuracy. Taking $p = 10$ or $p = 15$, the result for $\mathcal{H}_1(n)$ has to be the same, with the $\mathcal{H}_p(n)$ being evaluated by direct summation. These $\mathcal{H}_1(n)$ values can be divided by n and summed to give the quantity on the right in equation (41). Using the Mathematica routine FindFit we find the following expansion:

$$\sum_{k=1}^{n} \frac{\mathcal{H}_1(k)}{k} - \log(2)H_n = -\frac{0.00416808391164394962}{n^7} + \frac{0.01352090871752484971}{n^6}$$
$$-\frac{0.01366322081713273104}{n^5} - \frac{0.01347565742834329085}{n^4} + \frac{0.0729024264044047122}{n^3}$$
$$-\frac{0.1562495289343630581}{n^2} + \frac{0.2499999949068220114}{n} - 0.342014019497213398 \tag{48}$$

The negative constant in this expression when multiplied by two gives a value differing from the alternative estimate quoted above by 5×10^{-6}.

A third route to the negative constant leads in fact to an analytic result. It uses two expressions from Section 5 of the paper by De Doelder [26]:

$$\sum_{k=1}^{\infty} \frac{\psi(\frac{1}{2}(k+1)) - \psi(\frac{1}{2}k)}{k} = \frac{1}{6}\pi^2 + \log^2(2), \tag{49}$$

and

$$\sum_{k=1}^{\infty} (-1)^k \frac{\psi(\frac{1}{2}(k+1)) - \psi(\frac{1}{2}k)}{k} = -\frac{1}{6}\pi^2 + \log^2(2). \tag{50}$$

Adding these gives a sum over even k, leading to

$$\sum_{k=1}^{\infty} \frac{\psi(k+\frac{1}{2}) - \psi(k)}{k} = 2\log^2(2). \tag{51}$$

Taking into account the effect of replacing $\psi(k)$ by $\psi(k+1)$, the result is

$$\sum_{k=1}^{\infty} \frac{\psi(k+\frac{1}{2}) - \psi(k+1)}{k} = 2\log^2(2) - \frac{\pi^2}{6} = -0.6840280390118236\ldots \tag{52}$$

Hence, equation (43) is, leaving out terms tending to zero as $n \to \infty$:

$$\frac{(2n-1)\mathcal{C}_{2n-1,3}}{4} = 2H_{n-1}^2 + 8\log(2)H_{n-1} + 2H_{n-1}^{(2)} + 4\left[2\log^2(2) - \frac{\pi^2}{6}\right]. \tag{53}$$

In the asymptotic evaluation of $\mathcal{C}_{n,p}$ for p larger than three, sums arise which can be dealt with using the following result from [20]:

$$\sum_{k=1}^{n} \frac{H_k^{(2)}}{k} = H_n^{(2)}H_n - \sum_{k=1}^{n} \frac{H_k}{k^2} + H_n^{(3)}. \tag{54}$$
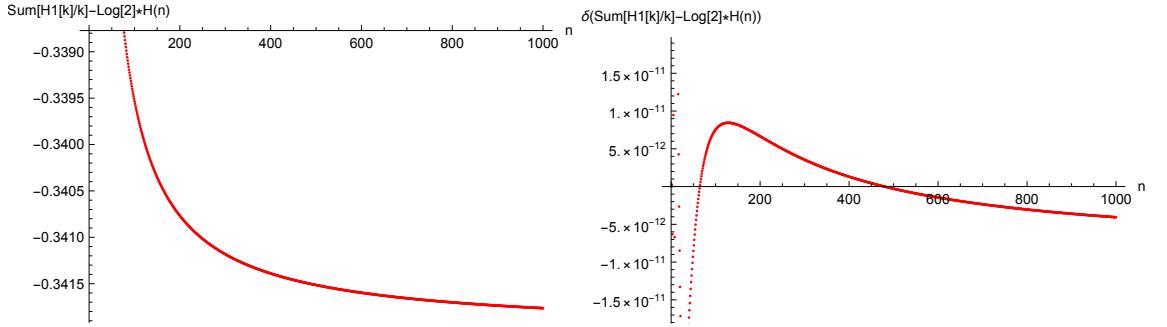
13

Figure 10: (Left) The values based on equation (46) for $\sum_1^n \mathcal{H}_1(k)/k - \log(2)H_n$ (blue) are compared with those from the fit function (48) (red). The two agree to high accuracy, as shown by the difference plot (right).

This is easily generalised to an arbitrary harmonic number of order p:

$$\sum_{k=1}^{n} \frac{H_k^{(p)}}{k} = H_n^{(p)} H_n - \sum_{k=1}^{n} \frac{H_k}{k^p} + H_n^{(p+1)}. \tag{55}$$

For $p = 1$, (55) reduces to (39).

The defining equation for the Stieltjes constants γ_n is:

$$\gamma_n = \lim_{m \to +\infty} \left[\sum_{k=1}^{m} \frac{(\log k)^m}{k} - \frac{(\log m)^{n+1}}{n+1} \right]. \tag{56}$$

A corresponding form of (55) is

$$\sum_{k=1}^{n} \frac{H_k^{(p)}}{k} - H_n^{(p)} H_n = H_n^{(p+1)} + \sum_{k=1}^{n} \frac{H_k}{k^p}, \tag{57}$$

and in the limit

$$\lim_{n \to \infty} \left[\sum_{k=1}^{n} \frac{H_k^{(p)}}{k} - H_n^{(p)} H_n \right] = \zeta(p+1) + \sum_{k=1}^{\infty} \frac{H_k}{k^p}, \tag{58}$$

for p positive.

Note that, from [19], the sum which occurs in (54) has the following asymptotic approximation

$$\sum_{k=1}^{n} \frac{H_k}{k^2} \sim 2\zeta(3) - \frac{2}{3}(\zeta(3) - H_n^{(3)}) - \frac{\log n}{n} - \frac{(1+6\gamma)}{n} + \frac{\log n}{2n^2} + \frac{(1+6\gamma)}{12n^2}. \tag{59}$$

As n goes to infinity, the sum tends to $2\zeta(3)$, in accordance with the first result below, with the other terms tending to zero. The last four terms on the right-hand side come from the use of the Euler-Maclaurin summation formula [19],

14

[25].The limiting values of a number for n going to infinity of other sums of this type are given in [24] and [22]:

$$\sum_{k=1}^{\infty} \frac{H_k}{k^2} = 2\zeta(3), \quad \sum_{k=1}^{\infty} \frac{H_k}{k^3} = \frac{\pi^4}{72} = \frac{5}{4}\zeta(4),$$

$$\sum_{k=1}^{\infty} \frac{H_k}{k^4} = 3\zeta(5) - \zeta(2)\zeta(3), \quad \sum_{k=1}^{\infty} \frac{H_k}{k^5} = \frac{7}{4}\zeta(6) - \frac{1}{2}\zeta(3)^2,$$

$$\sum_{k=1}^{\infty} \frac{H_k}{k^6} = 4\zeta(7) - \zeta(2)\zeta(5) - \zeta(4)\zeta(3). \tag{60}$$

Sums of this type have been studied since the time of Euler, with relatively recent results due to the late Jon Borwein and collaborators [27, 28] having been obtained using the techniques of experimental mathematics to complement analysis. Two of the sets of sums they consider are:

$$s_h(m, n) = \sum_{k=1}^{\infty} \frac{H_k^m}{(k+1)^n} \tag{61}$$

and

$$\sigma_h(m, n) = \sum_{k=1}^{\infty} \frac{H_k^{(m)}}{(k+1)^n}. \tag{62}$$

We define slight modifications of these:

$$\mathcal{I}_h(m, n) = \sum_{k=1}^{\infty} \frac{H_k^m}{k^n}, \quad \mathcal{J}_h(m, n) = \sum_{k=1}^{\infty} \frac{H_k^{(m)}}{k^n}. \tag{63}$$

Then [27]:

$$\mathcal{J}_h(m, n) = \sum_{k=1}^{\infty} \frac{H_k^{(m)}}{k^n} = \sigma_h(m, n) + \zeta(m+n), \tag{64}$$

and, in the special case $m = 2$ under particular investigation in [27, 28],

$$\mathcal{I}_h(2, n) = s_h(2, n) + 2s_h(1, n+1) + \zeta(n+2). \tag{65}$$

Euler provided the solution for $\sigma_h(1, m) = s_h(1, m)$ and consequently for $\mathcal{J}_h(1, m) = \mathcal{I}_h(1, m)$ for all $m \geq 2$:

$$\sigma_h(1, m) = \frac{m}{2}\zeta(m+1) - \frac{1}{2}\sum_{k=1}^{m-2} \zeta(m-k)\zeta(k+1). \tag{66}$$

Another useful relationship is the reflection formula, valid for $m, n \geq 2$:

$$\sigma_h(m, n) + \sigma_h(n, m) = \zeta(m)\zeta(n) - \zeta(m+n), \tag{67}$$

15

or

$$\mathcal{J}_h(m,n) + \mathcal{J}_h(n,m) = \zeta(m)\zeta(n) + \zeta(m+n), \tag{68}$$

so that $2\mathcal{J}_h(m,m) = \zeta(m)^2 + \zeta(2m)$ for $m \geq 2$.

Euler [28] was able to derive the following expansions in terms of zeta functions, for the particular case where the sum of parameters $s+t$ is odd, and $t > 1$. The first is for s odd, t even:

$$\sigma_h(s,t) = \frac{1}{2}\left[\binom{s+t}{s} - 1\right]\zeta(s+t) + \zeta(s)\zeta(t)$$
$$- \sum_{j=2}^{(s+t-1)/2}\left[\binom{2j-2}{s-1} + \binom{2j-2}{t-1}\right]\zeta(2j-1)\zeta(s+t-2j+1). \tag{69}$$

For s even, t odd:

$$\sigma_h(s,t) = -\frac{1}{2}\left[\binom{s+t}{s} + 1\right]\zeta(s+t)$$
$$+ \sum_{j=2}^{(s+t-1)/2}\left[\binom{2j-2}{s-1} + \binom{2j-2}{t-1}\right]\zeta(2j-1)\zeta(s+t-2j+1). \tag{70}$$

Table 5 of [27] gives a list of sums s_h for which the authors were unable to find representations in terms of zeta functions or zeta functions complemented by powers of logarithms of integers and polylogarithms of argument $1/2$, using various search algorithms. These results highlight the difficulty of finding closed form representations of all the Euler-type sums arising in treatments of the sums $\mathcal{C}_{n,p}$ for p large. Accordingly, we will adopt a less ambitious target of searching for representations of the $\mathcal{C}_{n,p}$ which involve a fixed number of the leading terms in expansions.

3   Leading order terms in the sums $\mathcal{C}_{n,p}$

We commence with the study of a class of sums over quotients H_k^{p-1}/k, both over a finite range from 1 to n, and the infinite range $n \to \infty$. The results for $p = 2$ have already been given in (39) and (60). The results for $p = 3$ are given in ([19]):

$$\sum_{k=1}^{n}\frac{H_k^2}{k} = \frac{1}{3}H_n^3 - \frac{1}{3}H_n^{(3)} + \sum_{k=1}^{n}\frac{H_k}{k^2}. \tag{71}$$

The method used to derive (71) employs Abel's summation formula and may easily be generalised to higher values of p. When this was done, a pattern

p	$\mathcal{D}_{p,q}$
2	1/2
3	-1/3, 1
4	1/4,-1,3/2
5	-1/5,1,-2,2
6	1/6,-1,5/2,-10/3,5/2
7	-1/7,1,-3,5,-5,3
8	1/8,-1,7/2,-7,35/4,-7,7/2
9	-1/9,1,-4,28/3,-14,14,-28/3,4
10	1/10,-1,9/2,-12,21,-126/5,21,-12,9/2
11	-1/11,1,-5,15,-30,42,-42,30,-15,5
12	1/12,-1,11/2,-55/3,165/4,-66,77,-66,165/4,-55/3,11/2
13	-1/13,1,-6,22,-55,99,-132,132,-99,55,-22,6
14	1/14,-1,13/2,-26,143/2,-143,429/2,-1716/7,429/2,-143,143/2,-26,13/2
15	-1/15,1,-7,91/3,-91,1001/5,-1001/3,429,-429,1001/3,-1001/5,91,-91/3,7
16	1/16,-1,15/2,-35,455/4,-273,1001/2,-715,6435/8,-715,1001/2,-273,455/4,-35,15/2

Table 1: The coefficients $\mathcal{D}_{p,q}$ in equation (72) for various values of p.

emerged for all the sums:

$$\sum_{k=1}^{n}\frac{H_k^{p-1}}{k} = \frac{1}{p}H_n^p + \mathcal{D}_{p,1}H_n^{(p)} + \sum_{q=2}^{p-1}\mathcal{D}_{p,q}\sum_{k=1}^{n}\frac{H_k^{q-1}}{k^{p-q+1}}. \tag{72}$$

Employing this pattern, it is easy to evaluate the coefficients $\mathcal{D}_{p,q}$ by choosing the same number of values of n as the number of unknowns, and solving linear equations for the $p-1$ unknowns. The values obtained can easily be checked for other values of n. Note that the coefficients in the linear equations are exactly known, and the values for the $\mathcal{D}_{p,q}$ are also exact. Some values are given in Table 1.

The lists of coefficients in Table 1 have some evident properties. The sum of the $\mathcal{D}_{p,q}$ over q when combined with $1/p$ from the first term on the right-hand side in equation (72) is required to be unity. For p even, $\mathcal{D}_{p,1} = 1/p$ and later coefficients show an even symmetry. For p odd, the sum of all $\mathcal{D}_{p,q}$ for $q \geq 2$ is required to be unity, and later coefficients show an odd symmetry. For p odd, the second coefficient in Table 1 is 1, while for p even it is -1.

We take the limit as $n \to \infty$ in equation (72) to define a set of harmonic sum Stieltjes constants γ_p^H, where:

$$\lim_{n\to\infty}\left[\sum_{k=1}^{n}\frac{H_k^{p-1}}{k} - \frac{1}{p}H_n^p\right] = \gamma_p^H, \tag{73}$$

and

$$\begin{aligned}
\gamma_p^H &= \mathcal{D}_{p,1}\zeta(p) + \sum_{q=2}^{p-1}\mathcal{D}_{p,q}\sum_{k=1}^{\infty}\frac{H_k^{q-1}}{k^{p-q+1}} \\
&= \mathcal{D}_{p,1}\zeta(p) + \sum_{q=2}^{p-1}\mathcal{D}_{p,q}\sum_{k=1}^{\infty}\mathcal{I}_{q-1,p-q+1}.
\end{aligned} \tag{74}$$

We have, using values of sums from [22, 23, 27, 28]:

$$\gamma_2^H = \frac{1}{2}\zeta(2) \approx 0.8224670334, \tag{75}$$

$$\gamma_3^H = \frac{5}{3}\zeta(3) \approx 2.0034281719, \tag{76}$$

$$\gamma_4^H = \frac{43}{8}\zeta(4) \approx 5.8174873812, \tag{77}$$

$$\gamma_5^H = \frac{79}{5}\zeta(5) + 3\zeta(2)\zeta(3) \approx 22.3153715822, \tag{78}$$

and

$$\gamma_6^H = \frac{729}{8}\zeta(6) + \frac{34}{3}\zeta(3)^2 \approx 109.0813822389. \tag{79}$$

The case $p = 7$ is more difficult, since not all necessary sums are given in the references [22, 23, 27, 28]. Zheng [22] gives $\mathcal{I}_h(1,6)$ and $\mathcal{I}_h(2,5)$, while $s_h(3,4)$, $s_h(4,3)$ and $s_h(5,2)$ are given in [27]. In order to use the latter set, we use the following generalisation of (65):

$$\sum_{k=1}^{\infty}\frac{H_k^n}{k^p} = \zeta(n+p) + \sum_{l=0}^{p-1}\binom{p-1}{l}s(p-l,n+l). \tag{80}$$

The following sums not given by Zheng have been obtained using (80):

$$\mathcal{I}_h(5,2) = \frac{2051}{16}\zeta(7) + \frac{57}{2}\zeta(5)\zeta(2) + 33\zeta(4)\zeta(3), \tag{81}$$

$$\mathcal{I}_h(4,3) = \frac{185}{8}\zeta(7) + 5\zeta(5)\zeta(2) - \frac{43}{2}\zeta(4)\zeta(3), \tag{82}$$

and

$$\mathcal{I}_h(3,4) = \frac{8}{33}\zeta(7) - \frac{2}{11}\zeta(5)\zeta(2) + \frac{10}{9}\zeta(4)\zeta(3). \tag{83}$$

Using these we find:

$$\gamma_7^H = \frac{946201}{3696}\zeta(7) + \frac{1967}{9}\zeta(4)\zeta(3) + \frac{1355}{22}\zeta(5)\zeta(2) \approx 647.5423438003. \tag{84}$$

By contrast with the Stieltjes constants, these harmonic sum coefficients are all positive, and increase immediately in rapid fashion, with those given here varying roughly as $(p-1)!$.

4 Evaluation and properties of the a_n

The Li coefficients a_n can be evaluated from the following expression [5]:

$$a_n = 2 \sum_{p=1}^{n} \mathcal{C}_{n,p} \Sigma_p^{\xi}. \tag{85}$$

As each quantity on the right-hand side of (85) is positive, then so are the a_n, as proved by Li [2].

The first 4000 values a_n have been calculated to 200 decimal places by direct summation, using the first 500 ξ_r values of Kreminski [12] (a sufficient number for this set). A table of these $\log a_n$ is available in ancillary material (see the ancillary file "logtabLian200500IV.csv"). A graph of the values is given in Fig. 11, together with their first differences. The latter are always positive, and decrease monotonically. They can be accurately fitted for $m \geq 100$ by a series of the form:

$$\log(a_{m+1}) - \log(a_m) = L_0 + \sum_{j=1}^{7} \frac{L_j}{(\log m)^j}. \tag{86}$$

Such a series with coefficients determined by FindFit yields errors bounded by ± 0.00005 for $m > 200$. Summing over the first differences gives the $\log a_n$ values, with Euler-Maclaurin summation giving accurate analytic approximations to the sums .
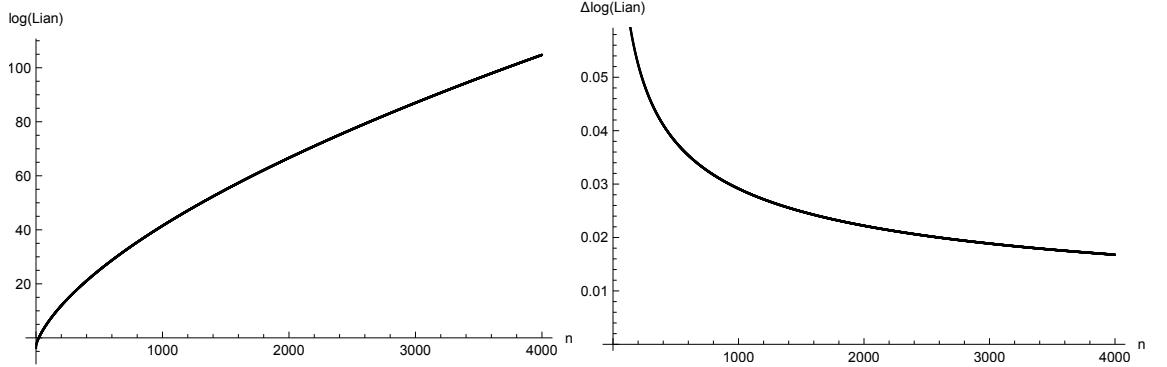

Figure 11: (Left) The first 4000 values of $\log a_n$. (Right) The difference between successive values of $\log a_n$.

The summand for the case $n = 4000$ is shown in Fig. 12. The Gaussian form of the summand is typical for large values of n.

One neat check on the numerical values of the a_n is to use them in the following particular case of their definition by Li [2]:

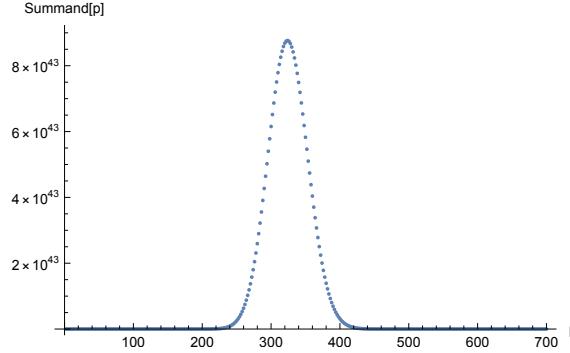$$2\xi(2) = 1 + \sum_{j=1}^{\infty} \frac{a_j}{2^j}. \tag{87}$$

19

Figure 12: The summand in the calculation of a_n for $n = 4000$.

This holds to all 200 digits of accuracy using summation over 1000 a_j's known to that accuracy. More generally, we can write the equivalent of (87) for arbitrary integers n:

$$2\xi(n) = 1 + \sum_{j=1}^{\infty} a_j \left(1 - \frac{1}{n}\right)^j. \tag{88}$$

Summing over 1000 values accurate to 200 digits, the accuracy falls rapidly as n increases: 2- 200 digits, 3- 158, 4- 107,5- 79,6- 61 etc. By $n = 29$, the summand maximum occurs at $j = 614$, and the summand has only fallen by a factor $1/e$ when $j = 952$. Note however that the convergence of the infinite series in (88) conveys useful information about the asymptotic behaviour of a_j: the quantity increases with j, but more slowly than $\exp(\alpha j)$ for any $\alpha > 0$. The leading terms on the left-hand side for n large and positive are:

$$1 + 2\sqrt{\frac{\pi}{n}} \left(1 + \frac{1}{6n} + O\left(\frac{1}{n^2}\right)\right) \exp\left(\frac{1}{2}(\log(n/(2\pi)) - 1)n\right). \tag{89}$$

A revealing check of tabulations of a_n values is to employ them to generate values for the sums λ_n^L or λ_n^K using equation (5). The results are shown in Fig. 13, together with the number of significant figures in the results from equation (2). The number of digits available in λ_n^K falls away from the initial 200 by around 4 for every increase of n by 50, so accuracy in the result is lost when n exceeds 2550. Keiper [1] gives a table of values of λ_n^K which can be used to validate the estimates arising from use of the a_n up to $n = 2000$. This test on the a_n values was satisfied to all available digits.

The data in Fig. 13 shows that for n large the equation (5) becomes ill-conditioned: on the right-hand side, the two terms to be subtracted get closer and closer, requiring more and more decimal places of accuracy in the a_n to give meaningful answers. This ill-conditioning has been commented on by other authors- e.g. [29, 30].

We deduced above an upper bound for a_n: the quantity increases with n, but more slowly than $\exp(\alpha n)$ for any $\alpha > 0$. We can easily bound the a_n
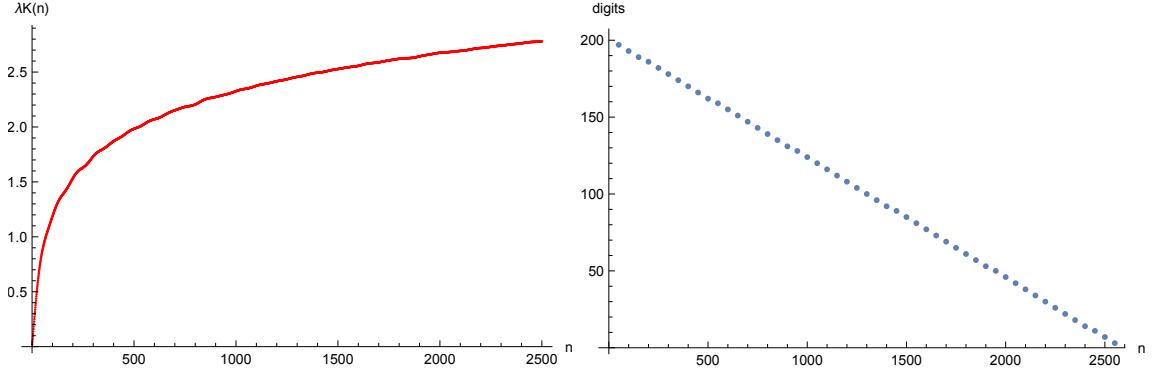
20

Figure 13: (Left) The first 2500 values of λ_n^K, calculated using equation (5). (Right) The number of significant figures in λ_n^K as a function of n .

from below, using the equation (85) and the fact that the sums Σ_p^ξ increase monotonically with p. We then have

$$a_n \geq 2\Sigma_1^\xi \sum_{p=1}^n \mathcal{C}_{n,p} = 8n\Sigma_1^\xi = na_1, \tag{90}$$

where $\sigma_1 = a_1 = 1 + \gamma/2 - \log(4\pi)/2 \approx 0.023095709$.

The recurrence relation (18) provides information about bounds on the $\mathcal{C}_{n,p}$ and consequently on the behaviour of the a_n. Firstly,

$$n\mathcal{C}_{n,p} - (n-2)\mathcal{C}_{n-2,p} = 4\mathcal{C}_{n-1,p-1} > 0 \implies n\mathcal{C}_{n,p} > (n-2)\mathcal{C}_{n-2,p}. \tag{91}$$

The quotient $\mathcal{C}_{n,p}/\mathcal{C}_{n-2,p}$ thus tends as $n \to \infty$ to a limit not smaller than unity. Secondly,

$$\mathcal{C}_{n,p} - \mathcal{C}_{n-2,p} = \frac{2}{n}(2\mathcal{C}_{n-1,p-1} - \mathcal{C}_{n-2,p}) \tag{92}$$

leads to

$$\mathcal{C}_{n,p} > \mathcal{C}_{n-2,p} \iff 2\mathcal{C}_{n-1,p-1} > \mathcal{C}_{n-2,p}. \tag{93}$$

4.1 Asymptotic treatment of the sum for the a_n

The summand in (85) contains terms for large p which consist of a Gaussian form for $\mathcal{C}_{n,p}$ and the exponential of the expression (14) for $\log \Sigma_p^\xi$. The $\mathcal{C}_{n,p}$ increase for small p, go through a maximum and then decrease. The Σ_p^ξ increase monotonically and strongly with p, and in consequence the summand in equation (85) has a maximum at a value $p_m^*(n)$ which lies after the maximum $B_o(n)$ of $\mathcal{C}_{n,p}$. Values of $p_m^*(n)$ and the logarithm of the maximum of the summand are given in Table 2. It will be noted that $p_m^*(n)$ increases far more rapidly with n than does $B_o(n)$. The consequence of this is that $p_m^*(n)$ moves further and further into the tail region of $\mathcal{C}_{n,p}$ as n increases.

21

n	$B_o(n)$	$p_m^*(n)$	$\log(max)$
500	13.7652	78	22.301593
1000	15.1461	126	38.449687
1500	15.9544	166	51.700331
2000	16.5281	202	63.315992
2500	16. 9732	236	73.832727
3000	17.3370	266	83.539034
3500	17. 6445	296	92.615928
4000	17.9110	324	101.182044

Table 2: The peak position $B_o(n)$ for $\mathcal{C}_{n,p}$ and the location $p_m^*(n)$ of the summand maximum for (5) together with its logarithm for various values of n.

In Fig. 14 we show the variation of $\log \mathcal{C}_{4000,2p}$ in the tail region, and compare it with the numerically determined fit function:

$$\log \mathcal{C}_{4000,2p} \approx -0.92012346 p \log p + 74.45559121. \tag{94}$$

The striking fact from this good fit in the region of p shown is that the lead term in (94) almost exactly cancels the leading term 0.920627926 in the fit for $\log \Sigma_p^\xi$ with p in the same range quoted just after the equation (14).

An analytic argument for such a cancellation between $\mathcal{C}_{n,p}$ and Σ_p^ξ contributions in the summand for a_n has been provided above in the discussion around the inequality (90). The possible $p \log(p)$ term in the exponent of the summand has to have a coefficient which is zero: the former contribution must then exactly cancel the latter.
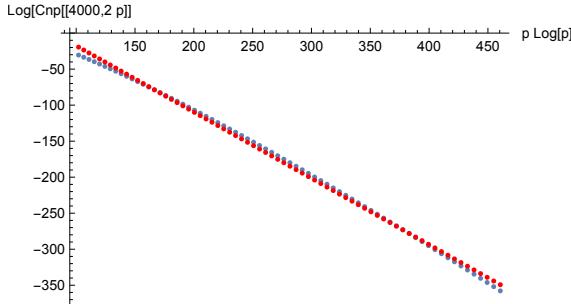

Figure 14: (Blue points) Values of $\log \mathcal{C}_{4000,2p}$ for various values of $p \log p$. (Red points) Values of the fit function (94).

The values of $B_o(n)$ in Table 2 increase as $2 \log(n)$, but the location $p_m^*(n)$ of the maximum of the summand for a_n has not as yet been determined by a simple formula. The maximum of the summand is given by the requirement that the derivative of the product $\mathcal{C}_{n,p} \Sigma_p^\xi$ be zero, or the derivatives of the two terms

$\log \mathcal{C}_{n,p}$ and $\log \Sigma_p^\xi$ add up to zero. In turn, these derivatives are to sufficient accuracy determined by differences of successive non-zero values of each. This criterion is exemplified in Fig. 15, for $n = 4000$. The $\mathcal{C}_{n,p}$ decrease more rapidly than the Σ_p^ξ increase in the relevant range, but the cancellation of leading terms means the first differences shown are much smaller than the values of each. This means that an analytic treatment to give a formula for $p_m^*(n)$ would have to have very accurate asymptotic formulae for each of the two terms.
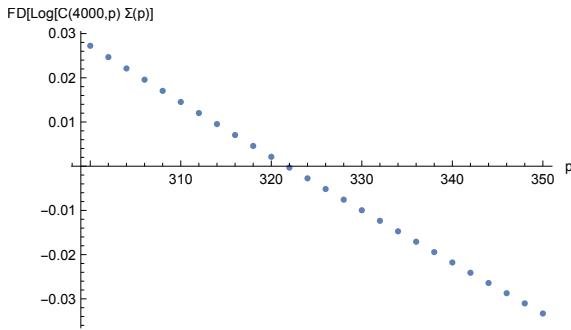

Figure 15: The first difference between successive non-zero values of $\log \mathcal{C}_{4000,p} \Sigma_p^\xi$ as a function of p.

Insight into the asymptotic form of $\mathcal{C}_{n,p}$ for large n and p comes from solving the partial differential equation (27). The solution is

$$\log \mathcal{C}_{n,p} \approx \log(n) + \mathcal{C}(p - 2\log(n)). \tag{95}$$

Here $\mathcal{C}$ is an arbitrary function. We investigate the following quadratic form:

$$\mathcal{C}(p - 2\log(n)) = \alpha(p - 2\log(n))^2. \tag{96}$$

This gives a representation with a maximum at $p = 2\log(n)$, which provides a reasonably good approximation to the data in Table 2, although of course much larger values of n are required to test this form.

One test of the fomulae (95) and (96) is provided in Fig. 16. Here accurate values of $\log \mathcal{C}_{n,p} - \log(n)$ for $n = 4000$ and $n = 2000$ when plotted with the abscissa $p - 2\log(n)$ lie close to the same curve in the region around $p = 2\log(n)$. However, what we are most interested in is the accuracy of the formula (96) in predicting the position $p_m^*(n)$ where the summand giving a_n has its maximum. As shown in Table 2, this occurs when $p >> 2\log(n)$.

The crucial result of further numerical tests is that, while the Gaussian form (96) is accurate for p close to $2\log(n)$, it gives p derivative values which are too negative to be compensated by the positive derivative values from the Σ_p^ξ for p around the values $p_m^*(n)$ of Table 2. Insight into this is provided by Fig. 17, which shows that the p derivative of $\log \mathcal{C}_{n,p}$ for large n can be divided into three regions when p exceeds $2\log n$: a steep fall away from the Gaussian
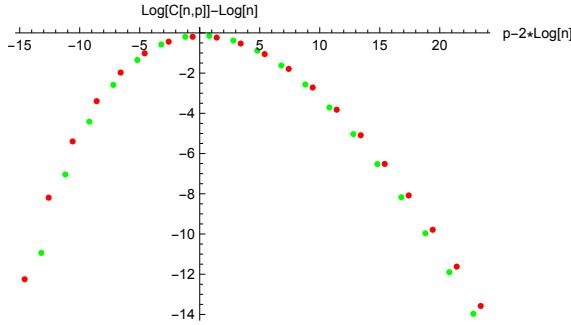
Figure 16: $\log \mathcal{C}_{n,p} - \log(n)$ as a function of $p - 2\log(n)$ for $n = 4000$ (red points) and $n = 2000$ (green points).

peak, a region of slower decrease, and then a steep decrease as p nears n. The maximum of the summand for a_n in fact occurs in the transition from the first to the second regions. The author has no analytic treatment explaining these numerical results.
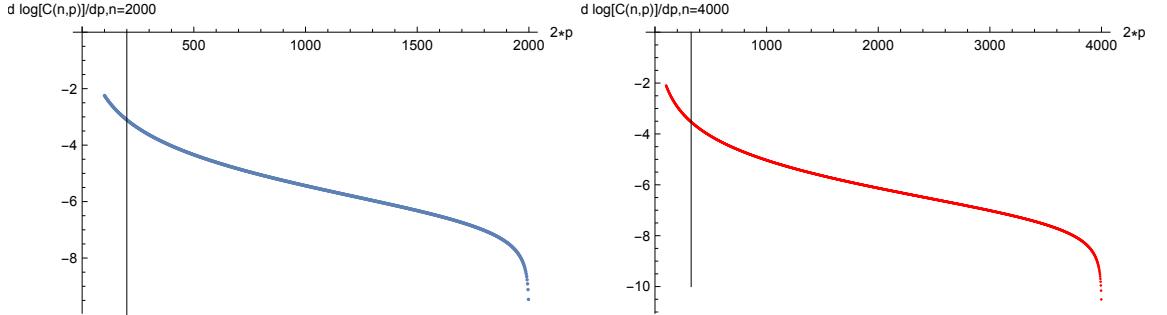

Figure 17: (Left) The difference between successive non-zero values of $\log \mathcal{C}_{n,p}$ for $n = 2000$ (left) and $n = 4000$ (right). The black vertical lines indicate the values $p_m^*(n)$ of Table 2 for these values of n.

4.2 A reformulation of Li's condition

An obvious reformulation of Li's necessary and sufficient condition for the Riemann hypothesis is provided by dividing both sides by na_n:

$$\frac{\lambda_n^L}{na_n} = 1 - \frac{1}{n}\sum_{j=1}^{n-1}\frac{\lambda_j^L}{a_j}\frac{a_j a_{n-j}}{a_n}. \tag{97}$$

Defining

$$\Lambda_n^L = \frac{\lambda_n^L}{a_n}, A_{n,j} = \frac{a_j a_{n-j}}{a_n}, \tag{98}$$

24

the equation (97 becomes

$$\frac{\Lambda_n^L}{n} = 1 - \frac{1}{n}\sum_{j=1}^{n-1} A_{n,j}\Lambda_j^L = 1 - \mathcal{S}_n. \tag{99}$$

The condition $\Lambda_n^L \geq 0$ is then equivalent to $\mathcal{S}_n < 1$. It has been verified that the iterative procedure (99) suffers from exactly the same ill conditioning as does that based on (5). Both generate for example the same answer with the same number of digits accuracy for $n = 2500$.

One important property of the $A_{n,j}$ is their symmetry:

$$A_{n,j} = A_{n,n-j}. \tag{100}$$

The $A_{n,j}$ then have a maximum for n fixed and j varying at $j = n/2$, with

$$max_j[A_{n,j}] = \frac{a_{n/2}^2}{a_n}. \tag{101}$$

Note that, from (90), if the Riemann hypothesis holds,

$$\frac{\Lambda_n^L}{n} = \frac{\lambda_n^K}{a_n} < \frac{\lambda_n^K}{na_1}. \tag{102}$$

The numerator having the leading term $(1/2)\log(n)$, the left-hand side tends down to zero as $n \to \infty$, at least as fast as $\log(n)/n$. The right-hand side sum in (97) consequently tends up to unity.

Consider next if the Riemann hypothesis fails. Using Keiper's formula [1]:

$$\lambda_m^K = \sum_{\rho}\left[1 - \left(\frac{\rho}{1-\rho}\right)^m\right], \tag{103}$$

there is then one or more zeros $\rho = \rho_*$ where $\rho_* = 1/2 + \delta_* + it_*$ where $0 < \delta_* < 1/2$ and from Platt and Trudgian [31] $t_* > 3 \times 10^{12}$. Combining such a ρ_* with its complex conjugate, their contribution to λ_m^K is of the form

$$\left(\lambda_m^K\right)_* \sim 2 - 2\left[1 + \frac{(1 + 4\delta_*^2)}{2t_*^2}\right]^{m/2}\cos\left(\frac{2m}{t_*}\right). \tag{104}$$

This contribution takes the form of an oscillation with slowly but exponentially increasing amplitude. The oscillatory function changes sign at intervals $\Delta m = t_*\pi/2$. The amplitude grows for large m as the exponential of $m(1 + 4\delta^2)/(4t_*^2)$. The lower bound ma_1 on the a_m grows as the exponential of $\log(m) - 3.7681$, and is therefore eventually exceeded by the amplitude term. For $t_* > 3 \times 10^{12}$ this occurs when $m \sim 10^{25}$.

We next consider a numerical fit to the curve of $\log(a_n)$ for n ranging from 100 to 4000. The following form works reasonably well:

$$\log(a_n) \approx A * n^p + B/n^{(1-p)}, \tag{105}$$

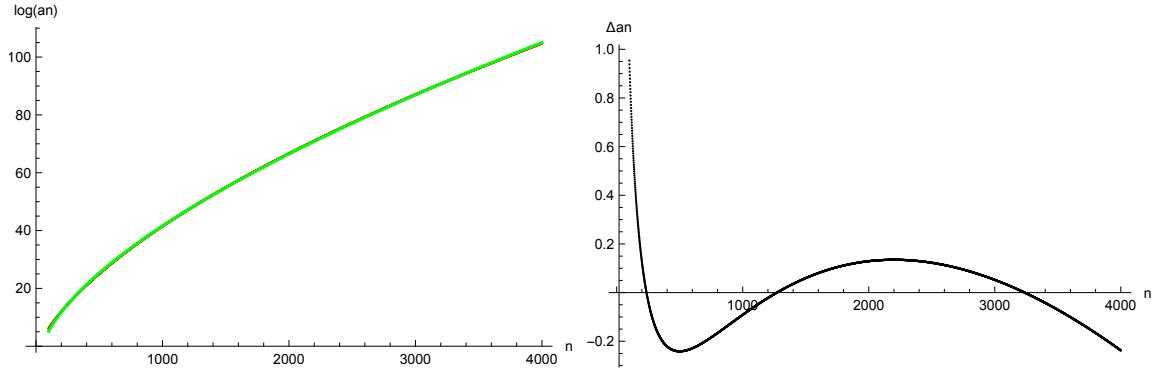where, from FindFit, $A \approx 0.52123852$, $B \approx -25.236314$ and $p \approx 0.641144106$.

Figure 18: (Left) The red curve shows the plot of $\log(a_n)$ as a function of n, while the green curve shows the fit function to it. (Right) The difference between the tabulated $log(a_n)$ and the fit function (105) is shown.

5 Conclusions

The investigations reported here complement those in the paper [5], and together suggest a technique for evaluating the Li constants a_n to high accuracy and for large values of n. Bounds on the a_n have also been given. Extension of the set of values given in the supplementary file to values of n in the range 10^5 and above would be valuable in making more accurate asymptotic expansions than those presented here, and perhaps enabling an improved understanding of the Keiper-Li criterion. At all events, the author hopes that some interesting new lines of research have been opened which may attract other investigators.

References

[1] Keiper, J.B. 1992 Power Series Expansions of Riemann's ξ Function *Math. Comp.* **58** 765-773.

[2] Li, X.J. 1997 The positivity of a sequence of numbers and the Riemann hypothesis *J. Number Th.* **65** 325–333.

[3] Voros, A. 2006 Sharpenings of Li's Criterion for the Riemann Hypothesis *Mathematical, Physics, Analysis and Geometry* **9** 53-63 .

[4] Coffey, M.W. 2010 On certain sums over the non-trivial zeta zeroes *Proc. R. Soc. A* **466** 3679-3692.

[5] McPhedran, R.C., Scott, T.C. and Maignan, A., 2022 Comments on and Extensions to Criteria of Keiper and Li for the Riemann Hypothesis *HAL Archive*, hal-03579652v1 and ACM Communications in Computer Algebra, **57**, pp. 85-110 (2023).

[6] Pustyl'nikov, L.D. 1999 On a property of the classical zeta-function associated with the Riemann hypothesis *Russian Mathematical Surveys* **54** 262–263.

[7] Pustyl'nikov, L.D. 2000 On the asymptotic behaviour of the Taylor series coefficients of $\xi(s)$ *Russian Mathematical Surveys* **55** 349–350.

[8] Hadamard, J.. 1893 Étude sur les propriétés des fonctions entiẽres et en particulier d'une fonction considéré par Riemann *Journal de Mathématiques Pures et Appliquées*, **9** 171–215.

[9] Gélinas J., private communication, 2021.

[10] Griffin, M., Ono, K., Rolen, L. and Zagier, D. 2019, Jensen polynomials for the Riemann zeta function and other sequences *Proc. Nat. Acad, Sci.*, **116**, 11103-11110.

[11] O'Sullivan, C. 2020 Zeros of Jensen polynomials and asymptotics for the Riemann ξ function http://arxiv.org/abs/2007.13582.

[12] Kreminski, R. 2003 Newton-Cotes integration for approximating Stieltjes (generalized Euler) coefficients *Math. Comp.*, **72**, 1379-97.

[13] Scott, T.C., Mann,R. and Martinez, R. 2006, General relativity and quantum mechanics: towards a generalization of the Lambert W function *A. A. E. C. C.*, **17**, 41-47.

[14] Maignan, A. and Scott, T.C., Fleshing out the generalized Lambert W function *ACM Communications in Computer Algnebra*, **52**, 45-60 (2016).

[15] O'Keeffe, M. 1995, Coordination sequences for lattices *Zeitschrift für Krystallographie*, **210**, 905-908.

[16] Conway, J.H. and Sloane, N.J.A. 1997, Low-dimensional lattices. VII Coordination sequences, *Proc. R. Soc. Lond. A*, **453**, 2369-2389.

[17] N.J.A. Sloane. The on-line encyclopedia of integer sequences.

[18] Wikipedia: Harmonic number.

[19] Mathematics Stack Exchange: Is there a closed form for $\sum_{k=1}^{n} H_{k-1}^2/k$?

[20] Mathematics Stack Exchange: Sum of powers of Harmonic Numbers.

[21] Wikipedia: Stieltjes constants.

[22] Zheng, D-Y 2007 Further summation formulae related to generalized harmonic numbers, *J. Math. Anal. Appl.*, **335**, 692-706.

[23] Choi, J. and Srivastava, H.M. 2011 Some summation formulas involving harmonic numbers and generalised harmonic numbers, *Math and Comp. Mod.*, **54**, 220-2234.

[24] Wenchang Chu 1997 Hypergeometric series and the Riemann zeta function, *Acta Arithmetica*,**82**, 103-118.

[25] NIST Handbook of Mathematical Functions, Cambridge University Press (2010),Chapter 2; Chapter 6.

[26] De Doelder, P.J. 1991 On some series containing $\psi(x) - \psi(y)$ and $(\psi(x) - \psi(y))^2$ for certain values of x and y, *J. Comp. and Appl. Math.*. **37**, 125-141.

[27] Bailey, D.H., Borwein, J.M. and Girgensohn, R. 1994 Experimental Evaluation of Euler Sums, *Experimental Mathematics*, **3**, 17-30.

[28] Borwein, D., Borwein, J.M. and Girgenshon, R. 1995 Explicit Evaluation of Euler Sums, *Proc. Edinb. Math. Soc.*, **38**, 277-294.

[29] Maslanka, K. 2004, Effective method of computing Li's coefficients and their properties, arXiv preprint, **math/0402168**.

[30] Voros, A. 2010, Sharpenings of Li's Criterion for the Riemann Hypothesis, *Mathematical Physics, Analysis and Geometry*, **9**, 53-63.

[31] Platt, D. and Trudgian, T. 2021, The Riemann hypothesis is true to 3×10^{12}, *Bulletin of the London Mathematical Society*, **53**, 792-797